ELECTRIC ARC FURNACE SLAG AND ITS USE IN HYDRAULIC CONCRETE

Idoia Arribas[a], Amaia Santamaría[b], Estela Ruiz[c], Vanesa Ortega-López[d] and Juan M. Manso[d]

[a] TECNALIA. c/Geldo – Parque Tecnológico de Bizkaia, Edificio 700 - 48160 Derio, SPAIN. E-mail: idoia.arribas@tecnalia.com

[b] Mining, Metallurgical and Materials Science Department, University of Basque Country, Alameda de Urquijo s/n, 48013 Bilbao, Spain. e-mail: amaia.santamaria@ehu.es

[c] LADICIM E.T.S. Ingenieros de Caminos, Canales y Puertos, University of Cantabria, Av/Los Castros s/n 39005 Santander Spain. e-mail: ruizes@unican.es

[d] Civil Engineering Department, EPS University of Burgos. Calle Villadiego s/n, 09001 Burgos, Spain. E-mail: vortega@ubu.es; jmmanso@ubu.es

Corresponding Author: Amaia SANTAMARIA. Engineering School of Bilbao. University of the Basque Country. 48013 Bilbao. Spain

Phone: 34-601-7319

e-mail: amaia.santamaria@ehu.es

Highlights

- Electric arc furnace oxidizing slag is a stony, rocky material used in construction and civil engineering, which shows some chemical changes and slight expansiveness over time.
- Collaboration between producers and consumers of electric arc furnace oxidizing slag is essential to guarantee good quality and homogeneous supplies, so that it may be efficiently re-used.
- Electric arc furnace oxidizing slag is a suitable aggregate for hydraulic cement concrete that forms a particular type of microstructure in the interfacial transition zone.

Abstract

Electric arc furnace oxidizing slag (EAFS) is a by-product of the steelmaking industry, generated after the melting and the preliminary acid refining of liquid steel. It is a stony material that is easy to crush for use as aggregate in concrete mixes.

This study examines the long-term aging reactions of EAFS and its volumetric stability, to gain further knowledge of this by-product, its behaviour as a construction material, and its inherent risk of swelling. Additionally, the good compressive strength of hydraulic mixes that incorporate this slag can be analyzed and explained on the basis of its steady and expansive compounds and its chemical evolution over time in the interfacial transition zone (ITZ); the appearance of calcium carbonate enhances the cohesiveness, stiffness and strength of this zone and, as a consequence, of the hydraulic concrete.

Keywords: electric arc furnace oxidizing slag, expansive compounds, slag weathering, accelerated aging, recycled aggregate, hydraulic concrete, interfacial transition zone, ITZ.

1. Introduction

The sustainability of human activity has become a key issue in the last decade of the 20th century and the first decade of the 21st century. The search for sustainability has driven the reuse of suitable industrial by-products with the right properties, thereby reducing the consumption of natural resources. Since the pioneering papers of Motz, Geiseler and Koros [1-3], almost all kinds of iron and steelmaking (as well as other metal) slags have been proposed for use in construction and civil engineering. Researchers now face the task of finding the most efficient and appropriate techniques for their reuse [4-20]. Several investigations on the re-use of steelmaking slags have been published over the last decades; some of them concerning mortar and concrete (rigid-stiff matrices) [21-43], and mixtures with granular soils (compliant-flexible and porous matrices) [44-58].

Electric arc furnace oxidizing slag (EAFS) is a by-product of the steelmaking industry, generated after the melting and the primary acid refining of liquid steel. Its chemical composition is based on its content of calcium, iron and silicon oxides in a global amount of over 80%; aluminium, magnesium, manganese and phosphorus oxides are also present. Variations in the proportion of these oxides are due to the kind of steel, the refractory materials of the furnace and some technological advances. In standard oxidizing

electric arc furnace slag (EAFS), the proportion of acid oxides (silica, alumina, iron oxide …) is predominant on the proportion of basic oxides (lime, magnesia and alkalis).

The similarity between the oxides, which may even be present in similar proportions in both EAFS and LD converter slag (Linz-Donawitz converter slag) or BOF-slag, (Basic Oxygen Furnace slag) and their common stony-gravel presentation, might lead to the erroneous impression that they are the same material. However, these products differ slightly, due the lower amount of free calcium oxide, CaO, also called free lime [59-68] in the EAFS, which also explains its lower expansiveness. Nowadays, the use of EAFS as a coarse aggregate in hydraulic concrete is widely accepted, while LD-slag is mainly applied in roadbeds. Maximum levels of volumetric expansion in materials used as concrete aggregates and as roadbedding are set at around 1% and 5%, respectively, in current standards.

Pioneering papers that detailed rigorous, systematic and global studies of the use of EAFS in mortar and concrete were published in Japan between 1991 and 1999 by K. Morino et al [69-71]; other publications in the same field over the same decade were less systematic. At the start of the 21st century, their work and those of other Japanese authors [72-74] were published in English, and several new research teams begin to work on this subject. Our team began its research in this field in 1997, beginning with the PhD Thesis of Prof. Manso; an initiative now exists among several EU research groups to establish pre-normative standards in this field.

The present study deals with EAFS expansion following spontaneous (weathering) and accelerated testing and, subsequently, its particular application as a coarse aggregate in hydraulic concrete. The composition and characteristics of EAFS are studied by means of standard analytical techniques: X-ray diffraction, thermogravimetric and differential calorimetric scanning analysis, low-vacuum SEM microscopy and EDX analysis. This article, based on the PhD Thesis of Ms Idoia Arribas, extends the results and adds subsequent findings from the research team. The long-term evolution of EAFS is studied, especially in terms of CaO migration, which is related to the characteristics of the Interfacial Transition Zone (ITZ) observed in the concrete mixes, leading to interesting results and relevant conclusions.

2. Background on EAFS

After cooling from 1580ºC, the EAFS by-product becomes a stony, cohesive, slightly porous, heavy, hard and tough material, the initial colour of which is almost black, due to the presence of iron oxides. Long-

56 term outdoor weathering causes its colour to change to clear-grey shades. It is easily crushed, its residual
57 metallic iron must be mostly separated, and it can then be employed as coarse and fine aggregate in
58 hydraulic mortars and hydraulic or bituminous concrete. Its other possible uses include bedding material
59 for roads and railways, and water depuration, as well as soil stabilization and correction.

60 All aggregate materials to be applied in concrete have to be analysed in depth before their use can be
61 standardized. Problems of alkali-aggregate reactions and intrinsic chemical instability are examples of the
62 risks associated with the use of certain natural minerals as aggregates. In the case of EAFS, an artificial
63 material, there is a general consensus that its chief problem is volumetric expansiveness or swelling of
64 pieces, lumps and particles, due to the chemical activity of expansive compounds such as free-CaO and,
65 sometimes, free MgO-periclase, an expansive compound that has scarcely been reported in the literature
66 [75]. Their presence is detrimental and should be carefully monitored when the concrete is prepared and
67 throughout its in-service life.

68 The main physical and chemical characteristics of EAFS for use as mortar and concrete aggregate, which
69 influence its weight and integrity, are its high density and its free calcium oxide content. Further relevant
70 characteristics have to be analysed and evaluated in its application, which require a wide range of
71 scientific analyses [76, 77]. The immediate effects of the addition of large amounts of EAFS aggregate
72 (on fresh and hard concrete) are loss of workability and an increase in the short-term mechanical
73 properties (strength at 7 and 28 days). These and other important questions (i.e. durability tests) have been
74 studied by the authors over the past decade and their results and opinions form part of the scientific
75 literature.

76 The main compounds of EAFS, according to the scientific literature, are single and complex calcium
77 silicates (containing aluminium or magnesium) and single and complex iron-based oxides (containing
78 calcium, magnesium, chromium, manganese, among others) which are in a liquid state above 1500ºC,
79 aided by fluxes such as CaF_2, which solidify at under 1200ºC. Silicates (dicalcium silicate β or γ belite-
80 larnite, ackermanite, gehlenite, wollastonite, calcium-olivine, kirschsteinite, melilite, and others) and iron-
81 based oxides (wustite, magnetite, hematite, dicalcium ferrite, R-O phase…) can be considered to add to
82 short-term stability, although their long-term chemical stability is not evident and has to be verified. The
83 undesirable presence of metallic iron in the slag must be eliminated through efficient magnetic separation.
84 Additionally, fresh EAFS slag (unweathered, after cooling) often contains small amounts of free-CaO

(also called free-lime) dispersed in its microstructure. Despite its presence, some of the analytical procedures to quantify its amount in the slag are unreliable. A more precise method of quantifying free-CaO content in EAFS is accelerated aging until total hydro-carbonation is achieved, followed by thermo-gravimetric heating analysis up to 900ºC.

Several reasons explain the volumetric instability of generic metallurgical slags. Firstly, the evolution of silicate β to γ is accompanied by an increase in volume, although this reaction is less likely in EAFS, due to the presence of P_2O_5 and other β-phase stabilizers. Secondly, the long-term oxidation of metallic iron from iron +2 to iron +3, although infrequent, has also been observed in metallurgical slags. Thirdly, it has been observed a low-temperature hydroxylation of free-CaO and subsequent carbonation, in the presence of moisture, and even of free-MgO, although the latter is uncommon in EAFS. These reactions are associated with a significant increase in volume, sometimes with short-term and at other times with long-term effects.

According to the scientific literature [61, 66], the free lime found in LD-slag can be divided into two groups. The first group is residual free lime (not completely dissolved in a liquid state) that is grainy or spongy with particle sizes of between 2 to 40 microns. The second group, precipitated free lime, is smaller than 4 μm and may be found in the grain boundaries of some iron-oxide- based compounds (dicalcium ferrite or R-O phase), either dispersed in the calcium silicates, in SC_3 crystals or in SC_2 crystals. Both are found in EAFS, although the latter are by far the most common.

Despite the fact that EAFS is an “oxidizing” slag, in which the predominant acid oxides are capable of dissolving all of the basic oxides, it is not uncommon to find some types of EAFS that contain undissolved particles of free-CaO. These particles are a consequence of the electric arc furnace procedure; partial addition of lime is sometimes made near the end of the “acid” refining process, without sufficient time for the other acid slag components to dissolve this lime. Finally, this free-CaO remains undissolved in the mass of the slag as it cools.

Furthermore, other operations such as the “foaming” of the slag in the electric arc furnace, the pouring process, and slag cooling method to room temperature all form part of the steelmaking process. There are at least two methods for cooling EAFS, from furnace temperatures to room temperature. One method is cooling in continuous mode, dousing a small flow of slag with water and obtaining particles, lumps and

pieces of a size under 40 mm; these particles may be used as gravel after metallic iron separation. The other method involves pouring the liquid slag into a large pit in a liquid state, depositing a new layer on the last layer of solidified slag, while several water jets cool the upper surface. The cooling rate of the slag in the latter case is lower than it is in the former case; thermal contraction and spontaneous shrinkage break up the slag into pieces of more than 40 mm in size, followed by subsequent crushing and metallic iron separation. The aforementioned operations determine very important aspects in the use of EAFS, such as in-solid-state porosity, density, metallic iron content, internal presence of cracks or crevices, and initial grading; these operations define the final quality of the EAFS for re-use in the construction and civil engineering sectors. Steelmaking procedure therefore has a central influence on the quality of the EAFS that is produced; in the past, steelmakers were not concerned with the quality of their slags as most of it was dumped in landfill sites. Nowadays, collaboration between the producers and the consumers of this material is essential and it would probably be an appropriate time to encourage such collaboration within the EU.

The density (ρ) of EAFS has been recorded within the range of 3 to 4 Mg/m^3. It depends mainly on the content of metallic iron ($\rho \approx 8$), iron oxides ($\rho \approx 5$) and the internal porosity. In construction and civil works, a higher density than ordinary concretes is sometimes required (marine-coastal blocks, retaining walls, foundations or great basement slabs), but it is sometimes compulsory to obtain as low a density as possible in the concrete, retaining the rest of its beneficial properties. In this case, a "slightly-lower-density EAFS" is desired, to decrease the concrete density until it reaches values close to those obtained when using natural siliceous or calcareous aggregates. The usual content of Fe-element in EAFS is between 20 and 30%, which implies an iron oxide content of 30 to 45% in weight; these values can be reduced in the steelmaking below 15-20% in Fe-element and below 22-30% in iron oxides. An additional porosity of about 5% in the EAFS will contribute to a reduction in its density with no detriment in its properties. It appears possible to reach values of between 3 to 3.2 Mg/m^3 in the density of EAFS without affecting steel and slag quality; in this case, the density of the resultant concrete (containing about 1800 Kg/m^3 of EAFS) can be kept below 2.6 Mg/m^3; 8% higher than conventional concrete. Subsequent use of suitable air-entraining additives in mixes can reduce the density even further to within the range of 2.5 to 2.6 Mg/m^3, which is a good value for the key strength-to-weight ratio of load-resistant materials.

3. The use of EAFS in hydraulic mixes up until the present and some new observations

Analyzing the role and the influence of EAFS used as aggregate in hydraulic mixes requires some investigation of the chemical interaction between EAFS, water and the cementitious matrix, including the presence of free-CaO. There is evidence of migration (diffusion of ions in aqueous solution) of this oxide from the core to the periphery of the aggregate pieces; periodic visual inspections of a stock-pile of EAFS exposed to weathering recorded changes in colour of the external surface material (associated with rainfall and its evaporation), from grey-black to grey-white. The white substance on the external surface was clearly calcium carbonate. The following was observed in relation to the migration of CaO.

Two relevant factors should be considered. Firstly, EAFS is gravel-like material the pieces of which contain pores, cracks and crevices from occluded gases in a liquid state at high temperature, variations in volume throughout cooling, the crushing process, and the initial hydration of the accessible free-CaO due to rainwater. Secondly, the dissolution of natural calcite that gives us the well-known geological forms of stalagmites and stalactites can explain the migration observed in EAFS stock-piles: accessible calcium oxide (free-CaO) added to rainwater and atmospheric carbon dioxide react to give soluble calcium bicarbonate $(CO_3H)_2$ Ca. The migration of this compound when dissolved in water to the surface of the external slag pieces or particles, and the subsequent evaporation of the water left the visible precipitation of white calcium carbonate. A fraction of the free-CaO might not be accessible to humidity and it should be noted that some of it may remain in an unreacted state, cloistered in the microstructure of the slag.

Moreover, when EAFS is used as aggregate in hydraulic mixes, there is a zone of the material, mortar or concrete, that is directly affected by the slow arrival of CaO, due to the aforementioned diffusion mechanism in the presence of humidity. This interfacial transition zone (ITZ), between the aggregate particles and the cementitious matrix, is considered a weak zone of the concrete. In this region, the appearance of micro-bleeding around the aggregate particles, porosity and some microstructural features depend on several factors, such as aggregate quality and size, the water-cement ratio, the binder and the age of the mix. The morphology and properties of the ITZ evolve at the same time as the hydraulic reactions of the Portland cement take place [78-82].

Following the excellent and exhaustive dissertation on the ITZ in the book of Metha and Monteiro [83], there have been few outstanding advances in the scientific literature. Several interesting works have been

published over recent years [78-82, 84-92] and, in general, it is accepted that the ITZ morphology-quality plays an important role in the global permeability and therefore the durability of hydraulic mixes, mortars and concretes. However, its influence on mechanical properties such as strength (tensile and compressive), stiffness and toughness have yet to be clearly established.

The ITZ has been described as a zone surrounding the aggregate particles and their contours of around 15 to 40 μm in size [80]. The main characteristics of this zone in the hard concrete have been identified as important porosity, a very high content of Portlandite, a presence of ettringite, and a lack of hydrated calcium silicates (S-C-H gel). Even the orientation of the Portlandite and ettringite crystals and the size of the neighbouring cement grains before the setting have been analysed. It is in fact accepted that the conditions of the fresh concrete and its setting and hardening strongly influence the resultant morphology and the state of the ITZ. Obviously, the long-term hydration of all cement particles (weeks, months) and the presence of Portlandite will promote slow and progressive changes in the morphology of this ITZ zone.

The water/binder ratio in the vicinity of the aggregate particles is notoriously increased in conventional concretes, compared to the average value in global concrete, which produces a porous ITZ. At this point, the behaviour of the EAFS in the presence of liquid water should be mentioned; in fact, there are only small amounts of capillary water on the surface of the EAFS pieces [81]. The ruggedness, the accessible porosity and the presence of hydrophilic (silicates) and hydrophobic (iron oxides) substances in the external contour of the slag pieces provoke a situation in which capillary water exists on the surface of EAFS, but not in abundance, and there is no bleeding due to gravity. The “wall effect” of common aggregate pieces, whether siliceous or calcareous, which produces an anomalous packing of cement particles in the vicinity of their surfaces, might be minimized in the vicinity of EAFS pieces. An ITZ depleted of large cement grains and with a scarce presence of small grains, is not evident in the EAFS aggregates, the surfaces of which do not repel the cement particles because of their similar components (silicates and oxides).

Therefore, the ITZ created in mixes that contain EAFS (in well performed mixes, with low effective water-to-cement ratios) at the end of the setting period, should differ from that of concretes that contain ordinary aggregates; this “new” ITZ will be smaller and less hollow than it is with natural rock aggregates. The slow migration of CaO from the core of the EAFS pieces to its surface, and its

subsequent chemical evolution to calcium carbonate, also affects the ITZ morphology. Hence, variations in the morphology and age-evolution of the ITZ around the EAFS pieces may be expected, accompanied by variations in the global properties of the concrete, such as its permeability, durability, and mechanical properties (tensile and compressive strength and stiffness).

The fracture surfaces of concrete specimens after mechanical tests, in which the larger aggregate pieces have detached themselves from the matrix, are widely accepted to be undesirable; on the contrary, when fracturing breaks and divides these coarse aggregate particles in a visible way, showing good adherence and cohesion between matrix and aggregate, the situation is encouraging. Some authors [81, 82] have observed a generally lower strength of the global concrete than of its components, aggregates (calcareous or siliceous) and cementitious matrix; they have explained this observation by a specific low-strength in the ITZ. Hence, it may be stated that the better the quality of the bond in the ITZ, the better the mechanical (tensile and compressive) strength of the concrete. In general, the concrete made with EAFS shows broken aggregate particles on the fracture surface after mechanical rupture testing, which is an evidence of a stronger ITZ; however, it should also be considered that the EAFS pieces have cracks and crevices in their mass, favouring breakage under lower loads.

Some studies [78, 81, 82] concluded that the porosity of the ITZ and the micro-cracks that extend out from the ITZ towards the cementitious matrix were the origin of general cracking in the concrete under strong external loading. This micro-cracking has frequently been observed in ordinary concretes under SEM microscopy and is attributed to differential deformations between aggregate and matrix under stresses, thermal variations and drying shrinkage. The aforementioned investigations stated that the existence of this interconnected and generalized micro-cracking can affect the mechanical strength of the mass of concrete and its transport properties.

The microscopic observations performed on EAFS mixes recorded no micro-cracks in the cementitious matrix surrounding the slag particles, though these particles show internal cracking; these EAFS concretes are, in general, less permeable than ordinary concrete [81]. When observations were conducted on the fracture surface of broken EAFS concretes after mechanical tests, only a few large cracks were observed, and the main crack broke the aggregate particle. No bleeding was noted by the authors of this study in the larger-sized concrete particles (larger than 1 mm) prepared with EAFS aggregate, nor has bleeding been noted in the literature [81, 93].

It was concluded that the ITZ explains the inelastic (non-linear) behaviour of concrete under loading-unloading cycles in compression tests [82], despite the fact that the present phases, aggregates and matrix, show a separate linear behaviour. Certainly, the stress-strain graph obtained with standard concretes tested under compression to failure shows a decreasing slope. However, when the EAFS mixes were tested under compression to failure, an almost-linear-elastic behaviour was observed in the load-strain graph [82]; hence, this effect is probably a further consequence of a singular ITZ, when the mixes are well-graded and they show high performance.

Finally, it should be stated that significant changes in the morphology of the ITZ will give rise to changes (although none too drastic) in the global properties of the concrete; as was observed in this case study.

4. Materials

4.1. Cement, water and natural aggregates

A Portland cement type I, as per ASTM C150 standard [94] with a chemical composition and particle fineness commonly found in ordinary concretes was used in this work. Mixing water was taken from the urban supply of the city of Bilbao, which showed a negligible amount of compounds that could affect the preparation of hydraulic mixes.

Siliceous fine aggregate of washed sand (from Arija – Burgos), sized between 0.1 and 1mm with a fineness modulus of 1.36 was used. The quartz particles were rounded, as revealed by the SEM images of mixes, with a specific gravity of 2.63 Mg/m^3.

Limestone aggregate, crushed and classified in three sizes (fine 0-5 mm, medium 5-12 mm and coarse aggregate 12-25 mm) was used. The chemical and physical characteristics are detailed in Table 1, and the specific gravity was 2.67 Mg/m^3.

Aggregate	EAFS1	EAFS2	Limestone
Fe_2O_3 (%)	30.8	27.54	0.34
CaO (%)	32.52	25.72	51.68
SiO_2 (%)	17.17	17.88	3.54
Al_2O_3 (%)	7.96	11.62	2.52
MgO (%)	4.56	3.82	0.64
MnO (%)	3.8	4.15	--
SO_3 Total (%)	0.25	0.01	0.39
$Na_2O + K_2O$ (%)	0.2	0.1	0.25

P_2O_5 (%)	0.58	0.46	--
TiO_2 (%)	0.59	0.71	0.05
Loss on ignition (%)	--	--	42.30
Porosity (%)	14.4	7.8	0.7
Water absorption (%)	7.37	3.35	0.52
Specific gravity (Mg/m^3)	3.01	3.32	2.67
X-Diffraction main compounds	Wustite-magnetite Ghelenite-Kirschsteinite(Mn), Chromite	Wustite-magnetite Larnite-Ghelenite Chromite	Calcite-dolomite minor

Table 1: Chemical composition (XRF) and other physical properties of aggregates

4.2. Electric arc furnace slag

Two types of crushed electric arc furnace slag (EAFS1 and EAFS2) were used in this study, as detailed in [35], supplied by two different steelmakers. Some images of EAFS1 (fresh and after long-term weathering) are shown in figure 1. Their global chemical composition and physical properties are detailed in the Table 1 and their grading followed the method described for the limestone aggregate. The slag samples from the steelmaker that produced the EAFS2 underwent slower cooling with greater evacuation of gases that resulted in lower porosity and water absorption, but with a higher specific gravity, unlike the EAFS1 slag that underwent a slightly different production process. Other factors that have an influence on slag density, such as the proportion of iron oxides and the metallic iron content, were similar in both slags. The results of X-ray diffraction in relation to the main crystalline components of the slag are also shown in Table 1.

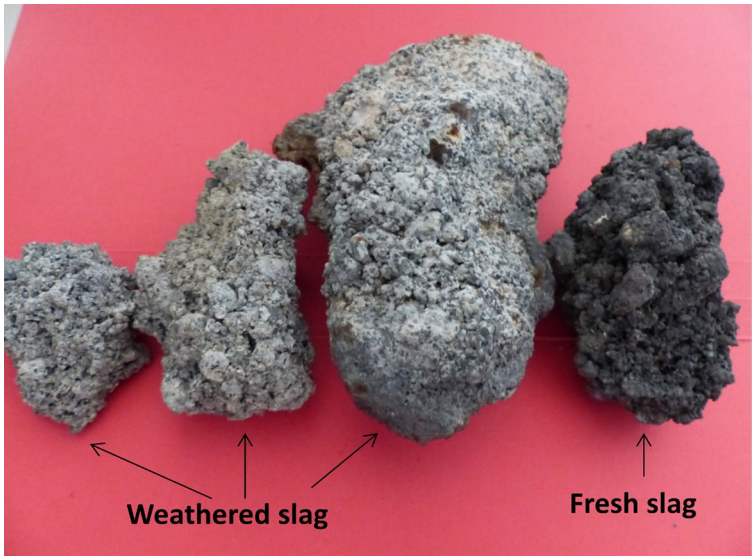

Figure 1 Fresh and long-term weathered EAFS1 slag.

4.3. Concrete preparation

Three concrete mixes were prepared, one of which was a reference concrete CR made using natural aggregates (crushed limestone and a minor proportion of siliceous sand), and the other two mixes had the same proportion of siliceous sand and two kinds of EAFS as aggregates, with the same grading and proportions as the limestone aggregate. Table 2 shows the main characteristics of these mixes, detailed, and discussed in a recent publication [35].

The matrix characteristics of these three mixtures, excluding the fine and coarse aggregates, should be the same, because their design is meant to be as similar as possible: the same cement content, the same fine fraction and water, similar plasticizer additives and the same volume and grading of coarse aggregate. The differences in the measured porosity analyzed by Mercury Intrusion Porosimetry (MIP) should come from the fine fraction of the EAFS included in the small samples.

Physical and mechanical tests were performed on these concretes yielding results that may be found in [35]; it should be added that the compressive strength after one year (long-term) reached a convergent value (about 62-65 MPa) for all of the concretes in this study. In the present article, an analysis of the EAFS particles and the ITZ found in these mixes is presented.

Mix Design	CEAFS1	CEAFS2	CR
CEM I 52,5 R (kg/m^3)	300	300	300
W/C	0.69	0.65	0.59
Slump (mm) with 3.5% additive	210	200	210
Fresh density (Mg/m^3)	2.8	2.96	2.51
Hardened density (Mg/m^3)	2.53	2.73	2.36
Compressive strength at 28-days (MPa)	55.0	55.7	40.8
Compressive strength at 90-days (MPa)	62.8	60.1	57.3
Porosity by MIP (%)	11.9	10.1	9.6

Table 2: Characteristics of the concrete mixtures.

5. Results of the EAFS characterization

The observation and analysis by means of SEM and EDX micro-analysis of polished samples of the hydraulic mixes, included in the following sections, provide relevant information on the structure and components of the EAFS in this study. Some images that illustrate the morphology of these components are shown in figure 2.

Samples of the slags were used to evaluate their dimensional stability in several states: as received without aging, after a period of three months of natural aging exposed to weathering and, finally after a period of more than five years in outdoor conditions. The tests were performed as per the ASTM D-4792 standard [94], submerged in water at 70ºC for over 2000 hours, and the results are shown in figure 3, with logarithmic ordinates for the sake of clarity. The results of potential expansiveness in the EAFS1 indicate an indispensable aging-weathering treatment of over two or three months for reliable use of this slag in the manufacture of concrete (expansion below1%). However, an eventual treatment similar to that proposed for EAFS1 slag is unnecessary for EAFS2 slag, as its expansion was under 1% in its "fresh-as received" state.

Furthermore, thermo-gravimetric and differential scanning calorimetric tests were performed on the samples after the aforementioned accelerated test. Figure 4 shows the results of these tests. As expected, the content of free-CaO in slags EAFS1 and EAFS2 was different and may be estimated at 2.5% in slag EAFS1 and at 0.2% in slag EAFS2. These estimates following hydration and carbonation and de-hydration and carbonate decomposition at 900ºC are largely reliable.

Figure 2. EAFS1 (upper) and EAFS2 (lower). The bands are one centimeter in length.

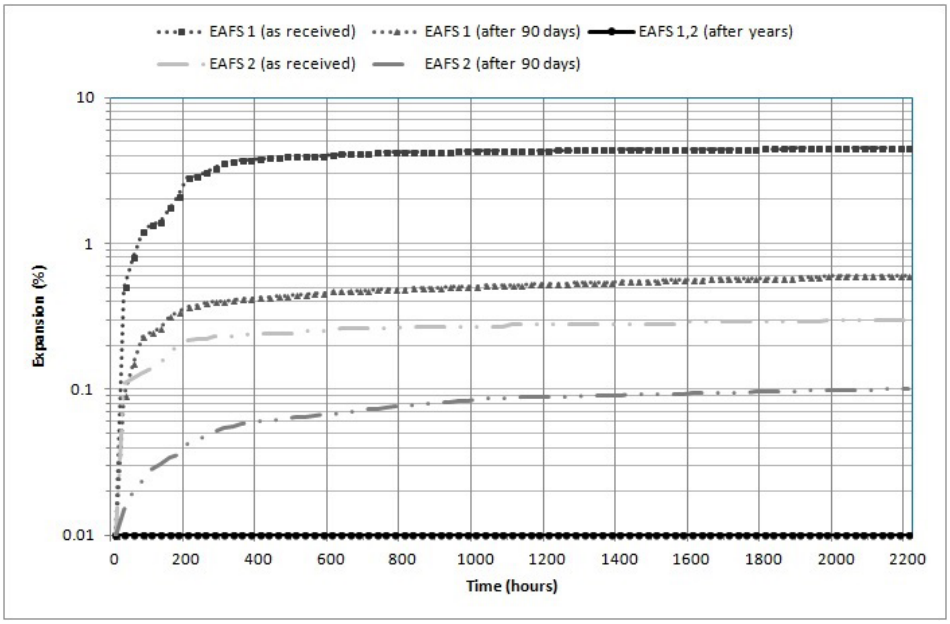

300

301 **Figure 3.-** Graph of slag expansiveness after ASTM D-4792 standard test.

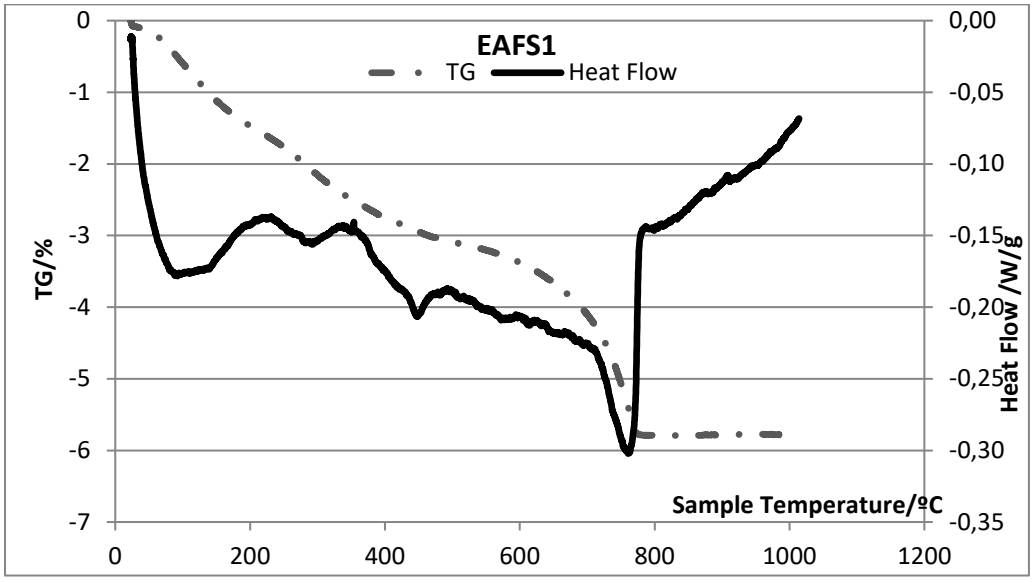

302

303 **Figure 4.** TG-DSC Graph of slags.

304 SEM observation and EDX analysis of both kinds of slag particles showed the appearance of the different
305 compounds or phases previously revealed in the XRD analysis. In figure 5, the main compounds and the
306 mapping of chemical elements throughout the image may be seen in slag EAFS1; a similar observation is
307 shown in figure 6 for EAFS2 slag. Aluminium, Iron and Chromium are the most significant elements to
308 identify the present phases.

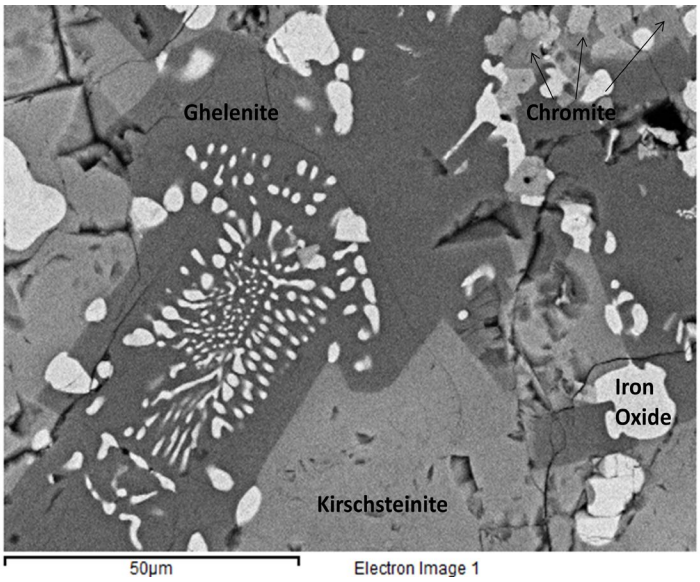

309

310 **Figure 5.** EAFS1 Microstructure and internal distribution of several chemical elements.

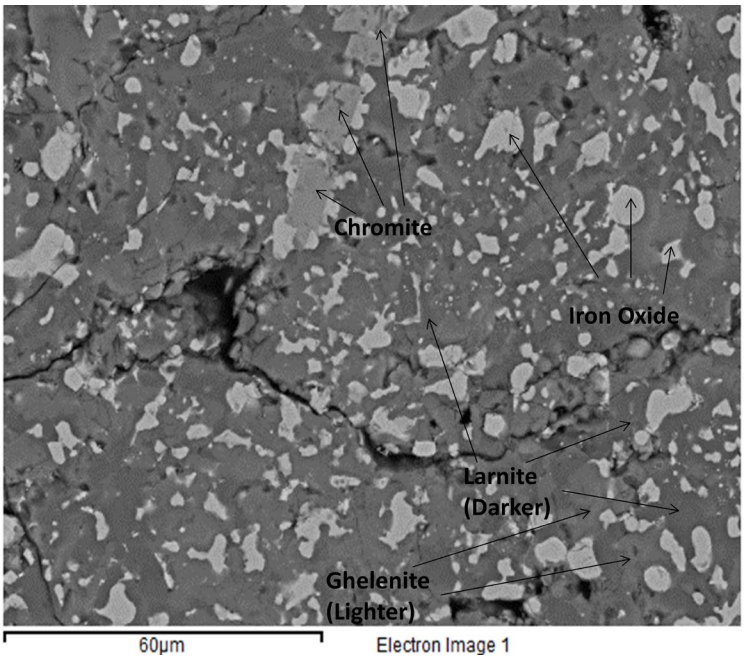

311

312 **Figure 6.** EAFS2 Microstructure and internal distribution of several chemical elements.

313 **6. Results of the ITZ analysis**

314 *6.1. SEM-EDX Analysis*

315 Following a detailed observation by SEM and the additional use of EDX-microanalysis of the hydraulic
316 mixes made with EAFS aggregate, outstanding differences were observed in the Interfacial Transition

Zone (ITZ). According to the literature [70], the ITZ has an extension of around 15-30 microns from the particles surface, but in the SEM image, Figure 7, a dark (black) “capillary-hole-crevice” with a width of 2-4 microns is visible along the contours of the natural aggregate particles.

In this figure 7, a particle of quartz-sand and another particle of EAFS1 are separated by the cementitious matrix in concrete CEAFS1; some internal cracks are visible in the slag particle. A more extended black hole-crevice may be seen in the contour of the sand particle than in the contour of the slag particle, in which some regions of its contour reveal no visible border (right-hand-side image) around the cementitious matrix. An image analysis program even makes it possible to evaluate the ratio length of the black hole-crevice-ITZ versus total contour length, for both kinds of particles; the numerical result is 78% in the sand particle and 32% in the slag particle. These values are the average from the measure of that ratio in three particles of each kind, sand and slag, in the two type of concrete.

It appears logical, on the basis of these observations, to think that about 78% of the external surface of the sand pieces have almost-null adhesion to the surrounding cementitious matrix; a value that is, on the contrary, far lower (32%) for the slag particle. The mechanical tests on this concrete yielded consistent results: on the fracture surface, the limestone and the sand-quartz pieces showed contours detached from the surrounding cementitious matrix and the appearance of the concrete in these areas, bordering the limestone and the sand zones, was very similar to the appearance of the external surfaces of the set concrete (wall effect). In contrast, the pieces of slag were broken on the fracture surface; which is once again quite logical, because the interfacial adherence with the matrix was better and the internal cracks assisted their breakage.

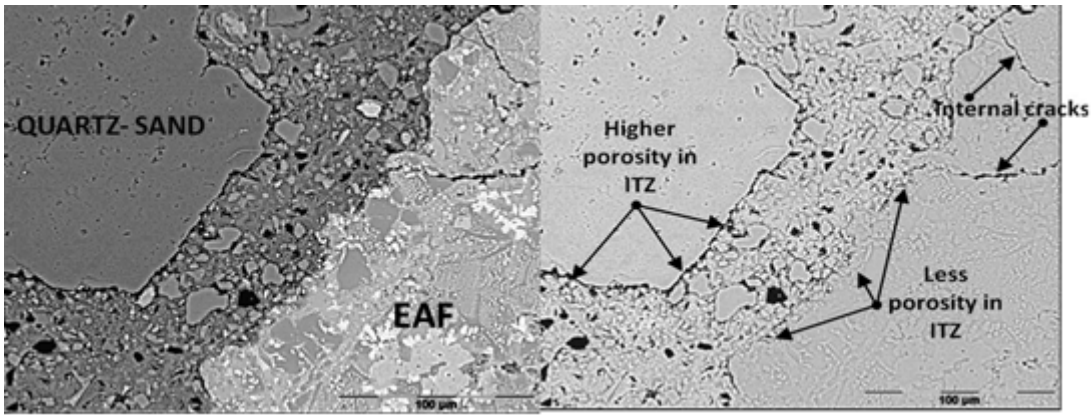

Figure 7. CEAFS1 microstructure (left). Image analysis of porosity in black colour (right).

A relevant image of concrete CEAFS2 is shown in figure 8. None or only a few holes may be observed in some zones of the slag particle contour (left); the border areas are full and fairly adherent. The most prominent detail is a band surrounding the slag aggregate which has the same grey shade as most of the smaller particles on the right; these smaller particles are fine-limestone aggregate. The EDX analysis revealed a band of almost-pure calcite with a width of 15-20 microns; as previously explained, this calcite is mainly from the free CaO of the slag. It could even partially come from the Portlandite, produced by the Portland cement, present in the vicinity of the cementitious matrix in the region of the ITZ, although this source is neither proven nor verified.

The situation described in figure 8 for the CEAFS2 is repeated in the SEM micrographs of concrete CEAFS1. It is more frequent in CEAFS1, as EAFS1 contains more free-CaO than EAFS2. However, the presence of calcite is only found on a small fraction of the contours of the slag particles and is not continuous along all particles.

Finally, the ITZ in the reference concrete CR is shown in figure 9, in which aggregate particles of siliceous sand and limestone are compared; in the second image the contours of both of these aggregates can be clearly observed, only a few of which are coherent with the cementitious matrix. Several hundred SEM images of all these concretes were taken in the course of this research and those included in this article are illustrative examples.

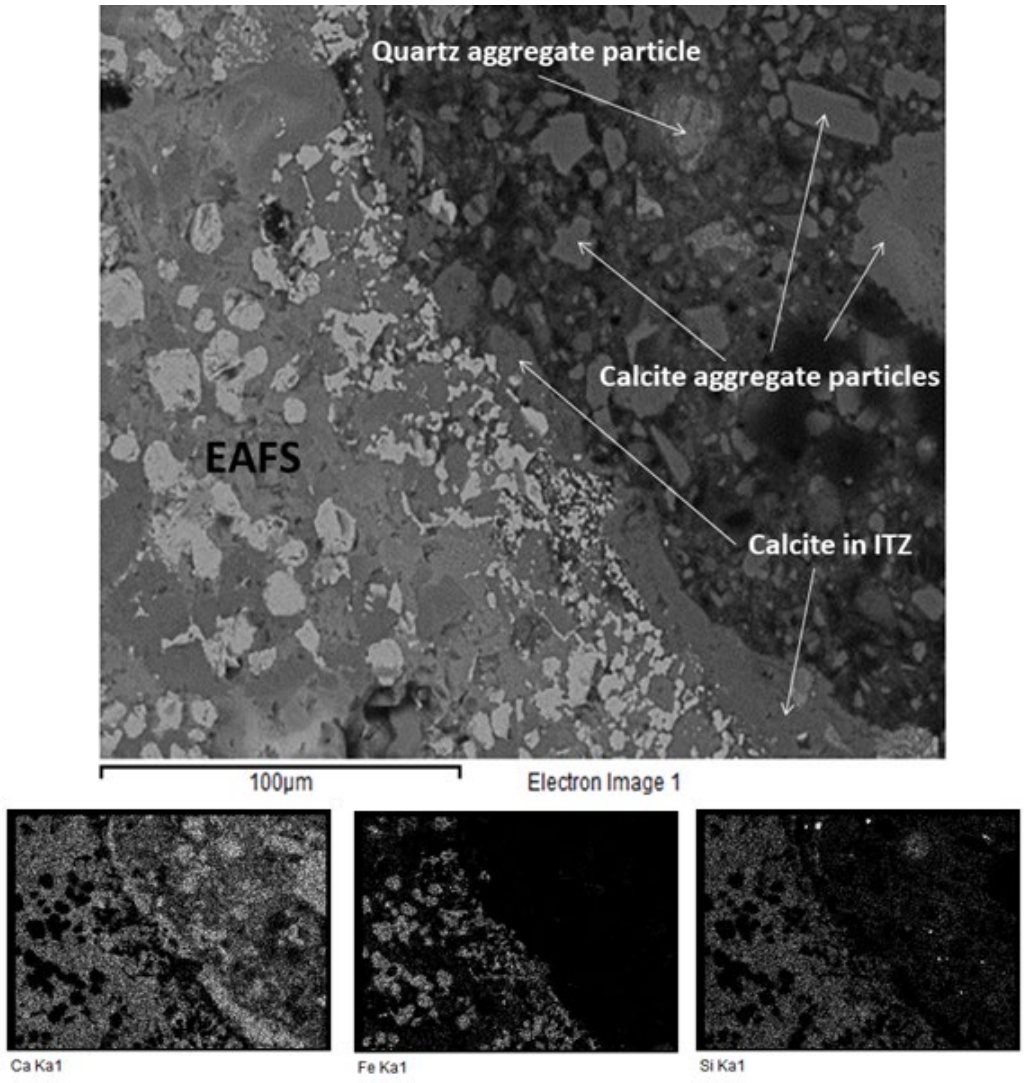

356

357 **Figure 8** SEM image of the microtexture of concrete CEAFS2

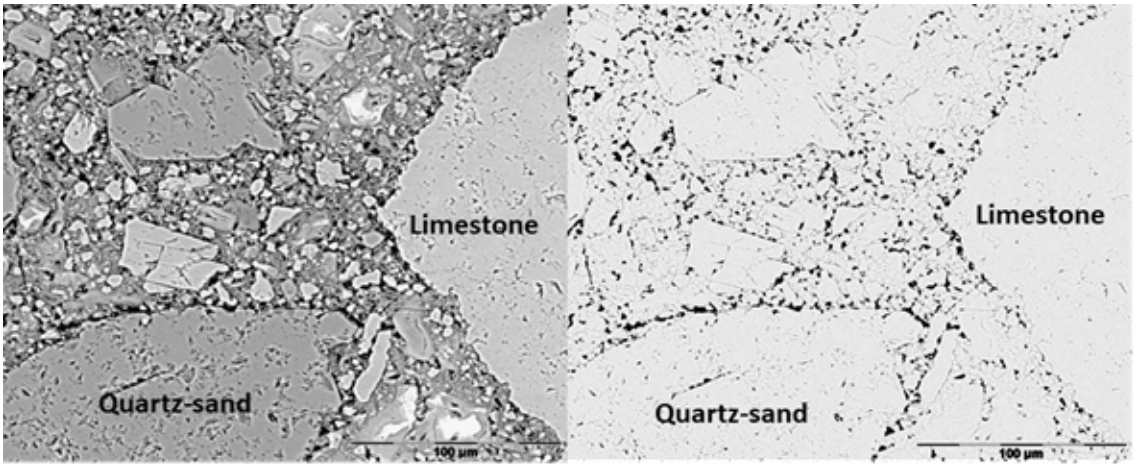

358

359 **Figure 9** SEM image of the microtexture of reference concrete CR

6.2. *Ultra-micro-indentation tests*

Ultra-micro-indentation tests (Shimadzu DUH-211) were performed on a concrete sample in the vicinity of the EAFS aggregate particles. A charge of 5N was used on a micro-indenter to obtain indentations of 1 to 5 microns. The indentation footprints were performed on a slag contour region in which the ITZ black-hole-crevice was almost inappreciable. The traces and the microstructure of the slag aggregate and the cementitious matrix were difficult to perceive in the optical microscopy images. The values obtained are shown in Table 3.

Mix Design	CEAFS1	CEAFS2	CR

Distance from slag Aggregate	Slag Aggregate	1-2 µm	5 µm	10 µm	15 µm	20 µm	25 µm
Series 1	1151	187	220	238	241	275	312
Series2	1034	194	212	245	245	245	295
Series3	825				254		

Distances in µm are measured from the contour of the particle to the surrounding matrix.

Table 3: Hardness values in MPa, measured from a slag particle to the cementitious matrix.

Doubts persist over the use of micro or nano-hardness values measured in a hollow-creviced region or in very porous region. Other authors [74,76] have published works in which such values are fixed and are represented in graphs in terms of the distance to the aggregate particles. In our case, the fall in hardness can be appreciated in the zone close to the slag particle contour (hole) in which values are slightly under 200 MPa; from a distance of 5 to 20 microns the values are almost-constant, and homogeneous values of around 300 MPa are only measured in the matrix at a distance of over 25 microns. Comparing these results with those obtained in the literature, it was concluded that the ITZ quality around the slag particles was excellent, and that the affected zone, within a radius of 25 microns, showed good level of hardness (240 MPa) compared to the hardness of the cementitious matrix.

6.3. *Compressive tests*

Load-unload tests were performed on the concrete mixes to estimate the elastic modulus and the linearity of the stress-strain relationship. The maximum load level was 60% of the 90-day compressive strength, assuming that the highest in-service stress of this material in a structure is around that value.

Mix Design	CEAFS1	CEAFS2	CR
Compressive strength at 28-days (MPa)	55.0	55.7	40.8
Compressive strength at 90-days (MPa)	62.8	60.1	57.3
60% Compressive strength at 90-days (MPa)	37.7	36.1	34.4
Elastic modulus at 28-days (GPa)	40.5	39.6	41.7
Elastic modulus at 90-days (GPa)	42.2	41.8	44.0

385 **Table 4:** Strength values of the concrete.

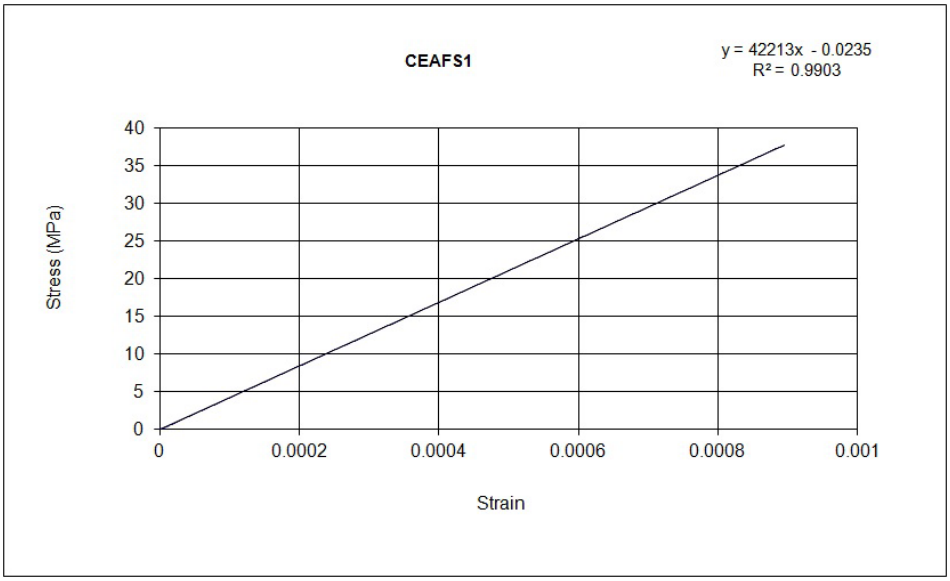

386

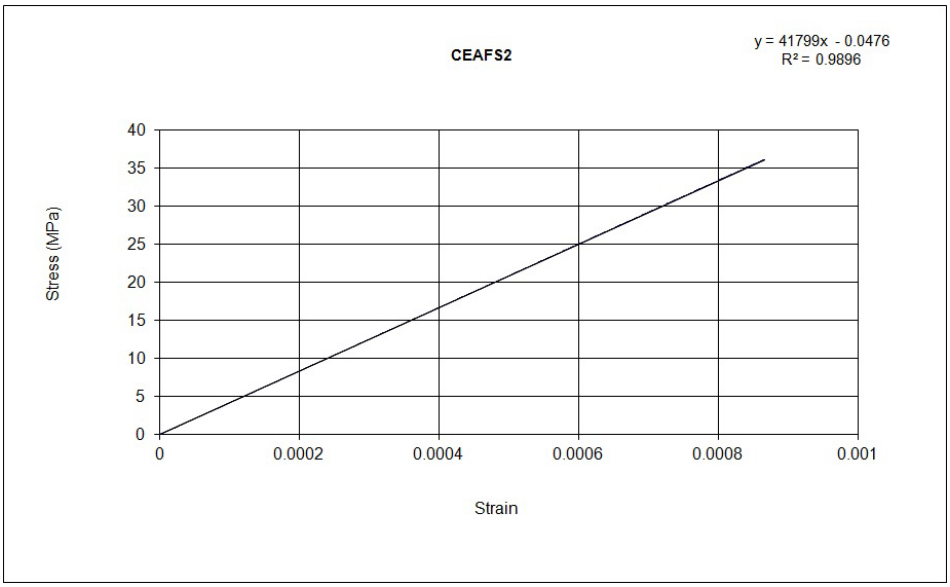

387

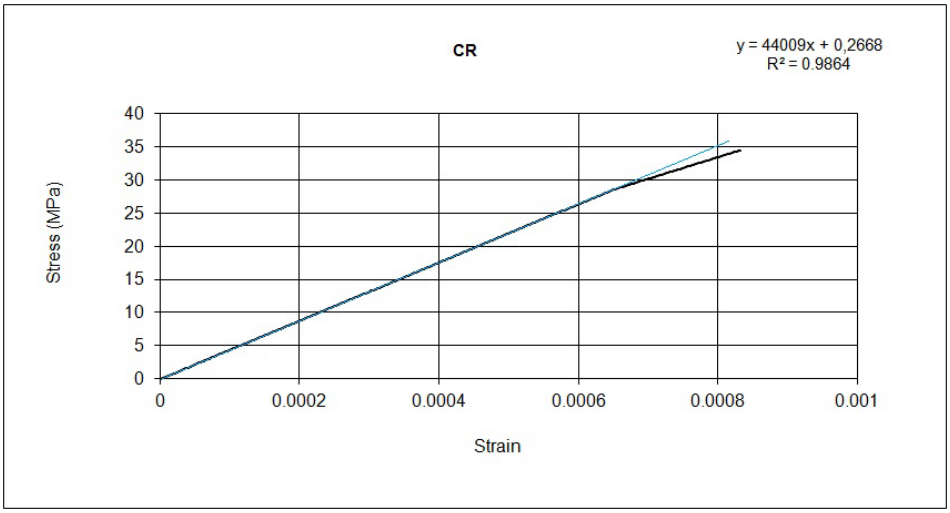

388

389 **Figure10.** Elastic moduli of the concretes

390 A good quality ITZ enhances the global elastic modulus and the straight linearity [81]. The results
391 showed a good linearity within the range of in-service loading for the EAFS slag concretes; the reference
392 concrete showed a small decrease in the slope of the curve at higher stress values could be attributed to a
393 lower quality ITZ that was subsequently affected by micro-cracking. However, the values of the elastic
394 moduli are slightly smaller in the EAFS concretes than in the reference concrete.

395 The quality and properties of the cementitious matrix in our concretes are very similar; hence, the
396 differences in the resultant elastic moduli are explained by the influence of the ITZ quality and the elastic
397 moduli of the aggregates. It is really difficult to establish a reference value for the Young's Modulus of
398 the electric arc furnace slag (its stiffness characteristics are highly scattered), but in this case the higher
399 porosity and the cracking state of the slag allow us to deduce that the elastic modulus of the natural
400 aggregates (used in the reference concrete) should be higher than the moduli of the EAFS. This effect is
401 stronger than the influence of the quality of the ITZ, and the elastic modulus is higher in the reference
402 concrete, the global results for which have been presented.

403 These results also provide evidence of the good quality and performance of the manufactured concretes
404 (300 kg of cement per cubic meter of concrete, with a global MIP porosity of 10%) and the excellent
405 mechanical behaviour of the ITZ of the EAFS slag concretes.

406 ## 7. Conclusions

407 Following the observations presented in this study it can be concluded that:

- The oxidizing electric arc furnace slag obtained after the manufacture of carbon steel, after suitable treatment, can and should be considered as an acceptable fine and coarse aggregate for the preparation of good quality concrete. Thus, relevant standards (or addendum to actual standards) should be prepared and published in the EU in the near future.

- The potential volumetric expansion of the electric arc furnace slag can be controlled and minimized during the production process in the factory.

- Among the particular characteristics of these slag concretes, the most important to be cited is a density of 5 to 20% higher than conventional concrete. The other characteristics are similar to those shown by the ordinary concrete.

- The performance of the tested slag-concrete mixtures is based on the reliable behaviour of the slag with regard to several technical aspects, especially its singular morphology in the matrix-slag aggregate interfacial transition zone (ITZ).

- The quality of the matrix-slag aggregate ITZ is better than the matrix-natural aggregate ITZ, enhancing the mechanical behaviour of the concrete.

Acknowledgements

The authors gratefully acknowledge funding from the Basque Regional Government in support of the research activities of Group IT 781-13. They would also like to thank staff from the University of Burgos and the University of Cantabria and employees of Hormigones y Minas S.A. and Hormor Zestoa S.L. for their collaboration with this research.

References

[1] Geiseler J. Use of steetwork slag in Europe. Waste Manage. 1996;16(1-3):59-63.

[2] Motz H, Geiseler J. Products of steel slags and opportunity to save natural resources. Waste Manage 2001;21(3):285-93.

[3] Koros PJ. Dusts, Scale, Slags, Sludges. . . Not Wastes, but Sources of Profits. Metall Mater Trans B 2003;34(6):769-79.

[4] Akinmusuru JO. Potential beneficial uses of steel slag wastes for civil engineering purposes. Resour Conserv Recy. 1991;5(1):73-80.

[5] Rubio AR, Carretero JG. La aplicación de las escorias de acería en Carreteras. Ingeniería Civil. 1991;80:5-9.

[6] Shelburne WM, DeGroot DJ. The use of waste and recycled materials in highway construction. Civil Eng Pract. 1998;13(1):5-16.

[7] San José JT. Reutilización y valoración en obra civil de escorias de horno eléctrico de arco producidas en la CAPV. Arte y Cemento. 2000;124(6):124-6.

[8] Papayianni I, Anastasiou E. Optimization of ladle furnace slag for use as a supplementary cementing material. In: Konsta-Gdoutos MS, editor. Measuring, Monitoring and Modeling Concrete Properties 2006. p. 411-7.

[9] Mäkikyro M. Converting Raw Materials into the Products - Road Base Materials Stabilized with Slag-based Binders. University of Oulu, Department of Process and Environmental Engineering Oulu: University of Oulu 951-42-7251-X (nid)/951-42-7252-8 (PDF): http://herkulesoulufi/isbn9514272528/ ISSN: 0355-3213: http://herkulesoulufi/issn03553213/. 2004.

[10] Yildirim IZ, Prezzi M. Use of Steel Slag in Subgrade Applications. Publication FWA/IN/JTRP-2009/32. Joint Transportation Research Program. West Lafayette, Indiana: Indiana Department of Transportation and Purdue University; 2009.

[11] DePree PJ, Ferry CT. Mitigation of expansive electric Arc furnace slag in Brownfield redevelopment. GeoCongress 2008: Geosustainability and Geohazard Mitigation. 178 ed. New Orleans, LA2008. p. 271-8.

[12] Papayianni I, Anastasiou E. Effect of granulometry on cementitious properties of ladle furnace slag. Cement Concrete Comp 2012;34(3):400-7.

[13] Serjun VZ, Mirtič B, Mladenovič A. Evaluation of ladle slag as a potential material for building and civil engineering. Materiali in Tehnologije. 2013;47(5):543-50.

[14] Setién J, Hernández D, González JJ. Characterization of ladle furnace basic slag for use as a construction material. Construct Build Mater. 2009;23(5):1788-94.

[15] Wang Q, Yang J, Yan P. Cementitious properties of super-fine steel slag. Powder Technol. 2013;245:35-9.

[16] García C, San José JT, Urreta JI. Reuse and valorization in civil works of electric arc furnace (EAF) slag produced in C.A.P.V. In: Gaballah I, Hager J, Solozabal R, editors. Global Symposium on Recycling, Waste Treatment and Clean Technology (REWAS 1999) Proc TMS Fall Extract Process Conf. San Sebastian1999. p. 417-24.

[17] San José JT, Uría A. Escorias de horno eléctrico de arco en mezclas bituminosas. Arte y Cemento. 2001;1905:122-5.

[18] Faleschini F, De Marzi P, Pellegrino C. Recycled concrete containing EAF slag: Environmental assessment through LCA. Eur J Environ Civ Eng. 2014;18(9):1009-24.

[19] Guo X, Shi H. Effects of steel slag admixture with GGBFS on performances of cement paste and mortar. Adv Cem Res. 2014;26(2):93-100.

[20] Qasrawi H. The use of steel slag aggregate to enhance the mechanical properties of recycled aggregate concrete and retain the environment. Constr Build Mater. 2014;54:298-304.

[21] Arribas I, San-José J, Vegas I, Hurtado J, Chica J. Application of steel slag concrete in the foundation slab and basement wall of the Tecnalia kubik building. 6th European Slag Conference Proceedings. Madrid, Euroslag 2010. p. 251-64.

[22] Fronek BA. Feasibility of expanding the use of steel slag as a concrete pavement aggregate: Cleveland State University; 2012.

[23] Manso JM, Polanco JA, Losañez Gonzalez M, Gonzalez JJ. Ladle Furnace Slag in Construction. J Mater Civil Eng. 2005;17:513-8.

[24] Bosela P, Delatte N, Obratil R, Patel A. Fresh and hardened properties of paving concrete with steel slag aggregate. Propiedades para firmes del hormigón fabricado con áridos siderúrgicos. Carreteras: Revista técnica de la Asociación Española de la Carretera. 2009;4(166):55-66.

[25] Abu-Eishah SI, El-Dieb AS, Bedir MS. Performance of concrete mixtures made with electric arc furnace (EAF) steel slag aggregate produced in the Arabian Gulf region. Construct Build Mater. 2012;34:249-56.

[26] Kim SW, Lee YJ, Kim KH. Bond behavior of RC beams with electric arc furnace oxidizing slag aggregates. J Asian Architect Build Eng. 2012;11(2):359-66.

[27] Nadeem M, Pofale A. Utilization of industrial waste slag as aggregate in concrete applications by adopting Taguchi's approach for optimizatio. Open J Civil Eng. 2012;2:96-105.

[28] Pellegrino C, Faleschini F. Experimental behavior of reinforced concrete beams with electric arc furnace slag as recycled aggregate. ACI Materials Journal. 2013;110(2):197-205.

[29] Pasetto M, Baldo N. Mix design and performance analysis of asphalt concretes with electric arc furnace slag. Constr Build Mater. 2011;25(8):3458-68.

[30] Papayianni I, Anastasiou E. Concrete incorporating highcalcium fly ash and EAF slag aggregates. Mag Concr Res. 2011;63(8):597-604.

[31] Anastasiou E, Georgiadis Filikas K, Stefanidou M. Utilization of fine recycled aggregates in concrete with fly ash and steel slag. Constr Build Mater. 2014;50:154-61.

[32] Etxeberria M, Pacheco C, Meneses JM, Berridi I. Properties of concrete using metallurgical industrial by-products as aggregates. Constr Build Mater. 2010;24(9):1594-600.

[33] Fronek B, Bosela P, Delatte N. Steel slag aggregate used in portland cement concrete. Transp Res Rec2012. p. 37-42.

[34] Pellegrino C, Cavagnis P, Faleschini F, Brunelli K. Properties of concretes with black/oxidizing electric arc furnace slag aggregate. Cem Concr Compos. 2013;37(1):232-40.

[35] San José JT, Vegas I, Arribas I, Marcos I. The performance of steelmaking slag concretes in teh hardened state. Mater Des. 2014;60:612-9.

[36] Arribas I, Vegas I, San-José JT, Manso JM. Durability studies on steelmaking slag concretes. Mater Des. 2014;63:168-76.

[37] Manso JM, Setién J. Investigación de nuevos usos de las escorias de horno eléctrico de arco (EAF): la oportunidad de los hormigones. Hormigón y Acero. 2006;241:51-7.

[38] Polanco JA, Manso JM, Setién J, González JJ. Strength and durability of concrete made with electric steelmaking slag. ACI Mater J. 2011;108(2):196-203.

[39] Manso JM, Hernández D, Losáñez MM, González JJ. Design and elaboration of concrete mixtures using steelmaking slags. ACI Mater J. 2011;108(6):673-81.

[40] Manso JM, Rodríguez A, Aragón A, Gonzalez JJ. The durability of masonry mortars made with ladle furnace slag. Constr Build Mater. 2011;25(8):3508-19.

[41] Manso JM, Gonzalez JJ, Polanco JA. Electric arc furnace slag in concrete. J Mater Civ Eng. 2004;16(6):639-45.

[42] Tarawneh SA, Gharaibeh ES, Saraireh FM. Effect of using steel slag aggregate on mechanical properties of concrete. Am J Appl Sci. 2014;11(5):700-6.

[43] Chinnaraju K, Ramkumar VR, Lineesh K, Nithya S, Sathish V. Study on concrete using steel slag as coarse aggregate replacement and ecosand as fine aggregate replacement. Intl J Res Eng Adv Tech. 2013;1(3).

[44] Manso JM, Ortega-López V, Polanco JA, Setién J. The use of ladle furnace slag in soil stabilization. Construct Build Mater. 2013;40:126-34.

[45] Petry TM, Little DN. Review of stabilization of clays and expansive soils in pavements and lightly loaded structures - History, practice, and future. J Mater Civil Eng. 2002;14(6):447-60.

[46] Montenegro J, Celemín-Matachana M, Cañizal J, Setién-Marquínez J. Ladle furnace slag in the construction of embankments: expansive behavior. J Mater Civil Eng. 2013;25(8):972-9.

[47] Kanagawa A, Kuwayama T. The improvement of soft clayey soil utilizing reducing slag produced from electric arc furnace. Denki Seiko. 1997;68(4):261-7.

[48] Ahnberg H, Johansson SE. Increase in strength with time in soils stabilised with different types of binder in relation to the type and amount of reaction products. Proceedings of the International Conference on Deep Mixing. Stockholm 2005. p. 195-202.

[49] Poh HY, Ghataora GS, Ghazireh N. Soil Stabilization Using Basic Oxygen Steel Slag Fines. J Mater Civil Eng. 2006;18(2):229-40.

538 [50] Yoon S, Balunaini U, Yildirim IZ, Prezzi M, Siddiki NZ. Construction of an embankment with a fly
539 and bottom ash mixture: Field performance study. J Mater Civil Eng. 2009;21(6):271-8.

540 [51] Yzenas JJ. The utilization of steel furnace slag for soil stabilization. 6th European Slag Conference
541 Proceedings. Madrid, Euroslag2010. p. 359-68.

542 [52] Chan C, Mizutani T, Kikuchi Y. Reusing dredged marine clay by solidification with steel slag: a
543 study of compressive strength. Int J Civ Struct Eng. 2011;2(1):270-9.

544 [53] Cheng T, Yan K. Mechanics properties of the lime-steel slag stabilized soil for pavement structures.
545 Adv Mater Res. 2011;168-170:931-5.

546 [54] Grubb DG, Wazne M, Jagupilla S, Malasavage NE, Bradfield WB. Aging effects in field-compacted
547 dredged material: Steel slag fines blends. J Hazard, Toxic and Radioactive Waste 2013;17(2):107-19.

548 [55] Kukko H. Stabilization of clay with inorganic by-products. Int J Civ Struct Eng. 2000;12(4):307-9.

549 [56] Mäkikyro M. Industrial slag use in geotechnical engineering: Slag in the geotechnical engineering
550 project. International conference on practical applications in environmental geotechnology ecogeo 2000
551 Geological Survey of Finland; Special Paper2001. p. 31-7.

552 [57] Mroueh UM, Eskola P, Laine-Ylijoki J. Life-cycle impacts of the use of industrial by-products in
553 road and earth construction. Waste Manage. 2001;21(3):271-7.

554 [58] Pasetto M, Baldo N. Cement bound mixtures with metallurgical slags for road constructions: Mix
555 design and mechanical characterization. Inzynieria Mineralna. 2013;14(2):15-20.

556 [59] Yildirim IZ, Prezzi M. Chemical, Mineralogical, and Morphological Properties of Steel Slag. Adv
557 Civil Eng. 2011;Article ID 463638:13. http://x.doi.org/0.1155/2011/463638.

558 [60] Goldring DC, Juckes LM. Petrology and stability of steel slags. Ironmak Steelmak. 1997;24(6):447-
559 56.

560 [61] Wachsmuth F, Geiseler J, Fix W, Koch K, Schwerdtfeger K. Contribution to the structure of BOF-
561 Slags and its influence on their volume stability. Can Metall Q. 1981;20(3):279-84.

562 [62] Geiseler J, Schlösser R. Investigation Concerning the Structure and Properties of steel Slags.
563 Proceedings of the 3rd International Conference on Molten Slags and Fluxes. Glasgow, Scotland 1988. p.
564 40-2.

565 [63] Juckes LM. The volume stability of modern steelmaking slags. T I Min Metall C. 2003;112(3
566 DEC.):177-97.

567 [64] Wang G, Wang Y, Gao Z. Use of steel slag as a granular material: volume expansion prediction and
568 usability criteria. J Hazard Mater. 2010;184 555-60.

569 [65] Mikhail SA, Turcotte AM. Thermal behaviour of basic oxygen furnace waste slag. Thermochim
570 Acta. 1995;263(C):87-94.

[66] Waligora J, Bulteel D, Degrugilliers P, Damidot D, Potdevin JL, Measson M. Chemical and mineralogical characterizations of LD converter steel slags: A multi-analytical techniques approach. Mater Charact. 2010;61(1):39-48.

[67] López FA, López-Delgado A, Balcázar N. Physico-chemical and mineralogical properties of EAF and AOD Slags. Afinidad LIII. 1996;53(461):39-46.

[68] Wang WC. Feasibility of stabilizing expanding property of furnace slag by autoclave method. Constr Build Mater. 2014;68:552-7.

[69] Morino K, Iwatsuki E. Durabiliy of concrete using electric arc furnace oxidizing slag aggregates. In: Swamy N, editor. Proc Int Conf. Sheffield1999. p. 213-22.

[70] Morino K, Iwatsuki E. Utilization of electric arc furnace oxidizing slag. In: Gaballah I, Hager J, Solozabal R, editors. Global Symposium on Recycling, Waste Treatment and Clean Technology (REWAS 1999) Proc TMS Fall Extract Process Conf. San Sebastian1999. p. 521-30.

[71] Morino K, Iwatsuki E. Properties of concrete using electric arc furnace oxidizing slag aggregates. In: Swamy N, editor. Second Int Conf on engineering materials. San José, California USA2001. p. 261-80.

[72] Hino M, Miki T. New role of steelmaking slags for the environmental protection of ocean. Shiraishi Memorial Lecture of teh Iron Institute of Japan. Tokyo2001. p. 44-5: 99.

[73] Sasamoto H, Tsubone A, Kamiya Y, Sano K. Development of fishing block using EAF refining slag. Tetsu To Hagane. 2003;89(4):461-5.

[74] Matsunaga H, Kogiky E, Tanishiki K, Nakagawa M. Environment-friendly block made from steel slag. ACI Special Publication SP. 2004;221(27):457-70.

[75] Frías M, San-José JT, Vegas I. Steel slag aggregate in concrete: The effect of ageing on potentially expansive compounds. Materiales de Construccion. 2010;60(297).

[76] Mäkelä M, Heikinheimo E, Välimäki I, Dahl O. Characterization of industrial secondary desulphurization slag by chemical fractionation with supportive X-ray diffraction and scanning electron microscopy. Int J Miner Process. 2015;134:29-35.

[77] Liapis I, Papayianni I. Advances in chemical and physical properties of electric arc furnace carbon steel slag by hot stage processing and mineral mixing. J Hazard Mater. 2014;283:89-97.

[78] Ollivier JP, Maso JC, Bourdette B. Interfacial transition zone in concrete. Adv Cem Based Mat. 1995;2(1):30-8.

[79] Elsharief A, Cohen MD, Olek J. Influence of aggregate size, water cement ratio and age on the microstructure of the interfacial transition zone. Cem Concr Res. 2003;33(11):1837-49.

[80] Scrivener KL, Nemati KM. The percolation of pore space in the cement paste/aggregate interfacial zone of concrete. Cem Concr Res. 1996;26(1):35-40.

[81] Maso JC. Interfacial Transition Zone in Concrete, RILEM Report 11. E&FN Spon, London1996.

[82] Scrivener KL, Crumbie AK, Laugesen P. The interfacial transition zone (ITZ) between cement paste and aggregate in concrete. Interface Science. 2004;12(4):411-21.

[83] Mehta PK, Monteiro PJM. Concrete: Microstructure, Properties, and Materials: McGraw-Hill Professional; 2013.

[84] Zimbelmann R. A contribution to the problem of cement-aggregate bond. Cem Concr Res. 1985;15(5):801-8.

[85] Gao Y, De Schutter G, Ye G, Tan Z, Wu K. The ITZ microstructure, thickness and porosity in blended cementitious composite: Effects of curing age, water to binder ratio and aggregate content. Compos Part B: Eng. 2014;60:1-13.

[86] Gao Y, De Schutter G, Ye G, Huang H, Tan Z, Wu K. Porosity characterization of ITZ in cementitious composites: Concentric expansion and overflow criterion. Constr Build Mater. 2013;38:1051-7.

[87] Gao JM, Qian CX, Liu HF, Wang B, Li L. ITZ microstructure of concrete containing GGBS. Cem Concr Res. 2005;35(7):1299-304.

[88] Mondai P, Shah SR, Marks LD. Nanoscale characterization of cementitious materials. ACI Mater J. 2008;105(2):174-9.

[89] Xiao J, Li W, Sun Z, Lange DA, Shah SP. Properties of interfacial transition zones in recycled aggregate concrete tested by nanoindentation. Cem Concr Compos. 2013;37(1):276-92.

[90] Li W, Xiao J, Sun Z, Kawashima S, Shah SP. Interfacial transition zones in recycled aggregate concrete with different mixiang approaches. Constr Build Mater. 2012;35:1045-55.

[91] Hashin Z, Monteiro PJM. An inverse method to determine the elastic properties of the interphase between the aggregate and the cement paste. Cem Concr Res. 2002;32(8):1291-300.

[92] Scrivener KL. Backscattered electron imaging of cementitious microstructures: Understanding and quantification. Cem Concr Compos. 2004;26(8):935-45.

[93] Arribas I. Ph Doctoral Thesis: Estudio y diseño de hormigones estructurales basados en la incorporación de subproductos siderúrgicos: viabilidad tecnológica; University of the Basque Country. Bilbao, Spain; 2013.

[94] Annual Book of ASTM Standards, ASTM International. West Conshohocken, 19429-2959. PA, USA2008.